

# Solid-State $^{113}\text{Cd}$ NMR Studies of Several Cadmium–Sulfur Complexes. Shielding Tensor–Structure Correlations

Joan Sola,\*† Pilar González-Duarte,\*† Jesús Sanz,‡ Isidre Casals,† Teresa Alsina,† Isabel Sobrados,‡ Angel Alvarez-Larena,§ Joan-Francesc Piniella,§ and Xavier Solans||

Contribution from the Departament de Química i Departament de Geologia, Universitat Autònoma de Barcelona, 08193 Bellaterra, Barcelona, Catalunya, Spain, Instituto de Ciencia de Materiales de Madrid, Serrano No. 115, 28006 Madrid, Spain, and Departament de Cristal·lografia, Mineralogia i Dipòsits Minerals, Universitat de Barcelona, Martí i Franquès s/n, 08028 Barcelona, Catalunya, Spain

Received January 19, 1993\*

**Abstract:**  $^{113}\text{Cd}$  CP/MAS-NMR spectra have been recorded for seven cadmium complexes including  $[\text{Et}_4\text{N}]_2[\text{Cd}_2(\text{SC}_6\text{H}_{11})_6]$  (1),  $[\text{Me}_4\text{N}][\text{Cd}(\text{S}_2\text{CSC}_6\text{H}_{11})_3]$  (2),  $[\text{Cd}(\text{SC}_3\text{H}_9\text{NHMe})_2][\text{ClO}_4]_2$  (3),  $[\text{Cd}\{\text{S}(\text{CH}_2)_3\text{NHMe}_2\}_2\text{X}_2]$  ( $\text{X} = \text{Cl}$  (4),  $\text{Br}$  (5)),  $[\text{Cd}_4\{\text{S}(\text{CH}_2)_2\text{NMe}_2\}_4\text{Br}_4]$  (6), and  $[\text{Cd}_4\{\text{S}(\text{CH}_2)_2\text{NMe}_2\}_6\text{Cl}_2]$  (7). Compounds 1 and 2 have been structurally characterized by X-ray crystallography. The former consists of discrete dinuclear  $[\text{Cd}_2(\text{SR})_6]^{2-}$  units containing  $\text{CdS}_4$  tetrahedral sites. The same coordination geometry is also present in polymeric complexes 3–5 with  $\text{CdS}_4$  (3) and  $\text{CdS}_2\text{X}_2$  ( $\text{X} = \text{Cl}$  (4),  $\text{Br}$  (5)) environments. Two different cadmium sites coexist in complexes 6 and 7, both formed by discrete tetranuclear molecules with  $\text{Cd}_4\text{S}_4$  rings. Coordination around cadmium is tetrahedral in  $\text{CdS}_2\text{Br}_2$  and  $\text{CdS}_2\text{N}_2\cdots\text{Br}_2$  sites of complex 6, a severe distortion toward octahedral geometry being present in the second site. In complex 7 there are an octahedral  $\text{CdS}_2\text{N}_2\text{Cl}_2$  environment and a highly distorted  $\text{CdS}_3\text{N}\cdots\text{Cl}$  center with a planar  $\text{CdS}_3$  moiety. The structure of 2 includes mononuclear  $[\text{Cd}(\text{SS})_3]^-$  anions, where the  $\text{CdS}_6$  coordination unit is distorted from a regular octahedron toward a trigonal prism. The shielding tensor, isotropic chemical shift ( $\sigma_{\text{iso}}$ ), chemical shielding anisotropy ( $\Delta\sigma$ ), and asymmetry parameter ( $\eta$ ) have been determined for all the sites. An orientation of the principal elements of the  $^{113}\text{Cd}$  shielding tensor is proposed for each cadmium environment. The magnitude of the tensor principal components in terms of the structural features around the cadmium atom is discussed as well as the variations of tensor elements in sites of close symmetry as a function of changes in the stereochemistry.

## Introduction

Solution  $^{113}\text{Cd}$  NMR studies were first to establish the basic features of the structure of rabbit liver metallothionein (MT) consisting of two distinct metal clusters:  $\text{Cd}_4(\text{S-Cys})_{11}$  and  $\text{Cd}_3(\text{S-Cys})_9$ .<sup>1</sup> Recent X-ray structure determination of  $\text{Cd}_5\text{Zn}_2$ -MT from rat liver<sup>2</sup> has confirmed the relevance of such studies and subsequent  $^{113}\text{Cd}$  NMR work on native metalated proteins.<sup>3</sup>

Nowadays, efforts are directed toward correlating the coordination stereochemistry of metal atoms in analogs for biologically occurring centers with shielding parameters derived from solid-state NMR studies. Thus, solid-state  $^{113}\text{Cd}$  and  $^{199}\text{Hg}$  NMR data have been related with M–thiolate complexes ( $\text{M} = \text{Cd}$ ,  $\text{Hg}$ ) of known structure<sup>4–6</sup> to serve as models for  $[\text{M}(\text{S-Cys})_n]$  and  $[\text{Cd}(\text{S-Cys})_2(\text{N-His})_2]$  centers in living systems. Similar studies concerning carboxypeptidase-A and thermolysin have been performed on cadmium complexes with nitrogen/oxygen coordination.<sup>7</sup> In some of these studies<sup>4,7</sup> the complete shielding tensor as well as its orientation with respect to a molecule fixed coordinate system has been derived from single-crystal NMR experiments.

Existing NMR data in model complexes for  $[\text{M}(\text{S-Cys})_n]$  centers are far more numerous for  $\text{M} = \text{Cd}$  than for  $\text{M} = \text{Hg}$ , mainly due to the large chemical shift anisotropies of the latter compounds, which render NMR signals difficult to observe. However, most of the solid-state or solution  $^{113}\text{Cd}$  NMR studies<sup>8</sup> have aimed at establishing a cadmium chemical shift scale as a function of the nature and geometry of coordinated donor atoms.<sup>9–11</sup> Indeed, studies relating the coordination geometry around cadmium nuclei with shielding tensor components are scarce and only referred to  $\text{CdS}_3$  trigonal,<sup>5</sup>  $\text{CdS}_2\text{N}_2$  tetrahedral,<sup>4</sup> and  $\text{CdO}_{(6-n)}\text{N}_n$ ,  $\text{CdS}_2\text{O}_4$ , and  $\text{CdSO}_3\text{N}_2$  octahedral coordination.<sup>7,12,13</sup>

With the aim of contributing to current information, we performed  $^{113}\text{Cd}$  solid-state NMR measurements on a series of cadmium–sulfur complexes, mainly with aminoalkanethiolate ligands, which span tetrahedral and octahedral coordination geometries and include  $\text{CdS}_4$ ,  $\text{CdS}_2\text{X}_2$ ,  $\text{CdS}_3\text{N}\cdots\text{Cl}$ ,  $\text{CdS}_2\text{N}_2\cdots\text{Br}_2$ ,  $\text{CdS}_6$ , and  $\text{CdS}_2\text{N}_2\text{X}_2$  centers. For each case the shielding parameters are related with bond angles and distances around the cadmium atom. The correlation works particularly well for tetrahedral coordination. Taking into account that zinc and calcium are spectroscopically silent metals which can easily be replaced by cadmium, data reported herein should be of use in

\* Departament de Química, Universitat Autònoma de Barcelona.

† Instituto de Ciencia de Materiales de Madrid.

‡ Departament de Geologia, Universitat Autònoma de Barcelona.

§ Universitat de Barcelona.

• Abstract published in *Advance ACS Abstracts*, September 15, 1993.

(1) Otvos, J. D.; Armitage, I. M. *Proc Natl. Acad. Sci. U.S.A.* **1980**, *77*, 7094.

(2) Robbins, A. H.; McRee, D. E.; Williamson, M.; Collett, S. A.; Xuong, N. H.; Furey, W. F.; Wang, B. C.; Stout, C. D. *J. Mol. Biol.* **1991**, *221*, 1269.

(3) Wüthrich, K. *Science* **1989**, *243*, 45.

(4) Santos, R. A.; Gruff, E. S.; Koch, S. A.; Harbison, G. S. *J. Am. Chem. Soc.* **1990**, *112*, 9257.

(5) Santos, R. A.; Gruff, E. S.; Koch, S. A.; Harbison, G. S. *J. Am. Chem. Soc.* **1991**, *113*, 469.

(6) Natan, M. J.; Millikan, C. F.; Wright, J. G.; O'Halloran, T. V. *J. Am. Chem. Soc.* **1990**, *112*, 3255.

(7) Rivera, E.; Kennedy, M. A.; Adams, R. D.; Ellis, P. D. *J. Am. Chem. Soc.* **1990**, *112*, 1400.

(8) Summers, M. F. *Coord. Chem. Rev.* **1988**, *86*, 43. Armitage, I. M.; Boulanger, Y. In *NMR of Newly Accessible Nuclei*; Laszlo, P., Ed.; Academic Press: New York, 1983; Vol. 2. Ellis, P. D. *Science* **1983**, *221*, 1141.

(9) Haberkorn, R. A.; Que, L., Jr.; Gillum, W. O.; Holm, R. H.; Liu, C. S.; Lord, R. C. *Inorg. Chem.* **1976**, *15*, 2408.

(10) Lacelle, S.; Stevens, W. C.; Kurtz, D. M., Jr.; Richardson, J. W., Jr.; Jacobson, R. A. *Inorg. Chem.* **1984**, *23*, 930.

(11) Dance, I. G.; Garbutt, R. G.; Craig, D. C. *Aust. J. Chem.* **1986**, *39*, 1449.

(12) Honkonen, R. S.; Marchetti, P. S.; Ellis, P. D. *J. Am. Chem. Soc.* **1986**, *108*, 912.

(13) Rodesiler, P. F.; Charles, N. G.; Griffith, E. A. H.; Amma, E. L. *Acta Crystallogr.* **1987**, *C43*, 1058.

Table I. Crystallographic Parameters

	[Et <sub>4</sub> N] <sub>2</sub> [Cd <sub>2</sub> (SC <sub>6</sub> H <sub>11</sub> ) <sub>6</sub> ] (1)	[Me <sub>4</sub> N][Cd(S <sub>2</sub> CSC <sub>6</sub> H <sub>11</sub> ) <sub>3</sub> ] (2)
formula	C <sub>52</sub> H <sub>106</sub> N <sub>2</sub> S <sub>6</sub> Cd <sub>2</sub>	C <sub>25</sub> H <sub>45</sub> NS <sub>3</sub> Cd
molecular weight	1176.6	760.6
a, Å	17.642(4)	16.943(2)
b, Å	14.034(3)	11.681(6)
c, Å	12.158(3)	19.384(4)
α, deg	90	90
β, deg	100.50(3)	108.86(1)
γ, deg	90	90
V, Å <sup>3</sup>	2960(2)	3630(2)
Z	2	4
F(000)	1248	1576
d <sub>calc</sub> , g·cm <sup>-3</sup>	1.320	1.392
crystal system	monoclinic	monoclinic
temp	ambient	ambient
space group	P2 <sub>1</sub> /a (No. 14)	P2 <sub>1</sub> /c (No. 14)
radiation	Mo Kα (λ = 0.710 73)	Mo Kα (λ = 0.710 73)
crystal size, mm	0.12 × 0.12 × 0.1	0.6 × 0.35 × 0.15
linear abs coeff, cm <sup>-1</sup>	9.51	11.13
scan mode	ω/2θ	ω/2θ
2θ max, deg	50	50
no. of unique reflns	3456	6375
no. of obsvns (I > 2.5 σ(I))	2364	4492
no. of variables	290	327
largest residuals, e·Å <sup>-3</sup>	0.4/-0.3	0.92(near to Cd)/-0.36
R	0.065	0.043
R <sub>w</sub>	0.070	0.049

the study of spectroscopic features not only of cadmium but also of zinc and calcium centers in living systems.

### Experimental Section

**Preparation of Compounds.** [Et<sub>4</sub>N]<sub>2</sub>[Cd<sub>2</sub>(SC<sub>6</sub>H<sub>11</sub>)<sub>6</sub>] (1). The following reaction was carried out under nitrogen atmosphere using standard Schlenk techniques and dry solvents. A solution of CdCl<sub>2</sub> (0.183 g, 1 mmol) in 20 mL of methanol was added slowly to a stirred methanolic solution (15 mL) of HSC<sub>6</sub>H<sub>11</sub> (0.38 mL, 3.0 mmol) containing an equimolar amount of NaMeO. Then, Et<sub>4</sub>NCl (0.166 g, 1.0 mmol) in ca. 10 mL of MeOH was added. After 2.5 h, the solvent was removed *in vacuo* and the solid residue was treated with hot CH<sub>3</sub>CN (50–60 °C). Filtration of the hot solution allowed separation of NaCl. Slow evaporation of the filtrate gave a colorless microcrystalline solid, which was filtered, washed in ether, and dried *in vacuo*. Yield: 0.412 g (70%). Calcd for C<sub>52</sub>H<sub>106</sub>N<sub>2</sub>-Cd<sub>2</sub>S<sub>6</sub>: C, 53.08; H, 9.08; N, 2.38; S, 16.35. Found: C, 53.08; H, 9.07; N, 2.33; S, 16.40. [Me<sub>4</sub>N]<sub>2</sub>[Cd<sub>2</sub>(SC<sub>6</sub>H<sub>11</sub>)<sub>6</sub>] (1') was synthesized in a similar manner in 75% yield. Both (1) and (1') were kept under nitrogen so that they would not decompose to give insoluble polymeric species of formula [Cd(SC<sub>6</sub>H<sub>11</sub>)<sub>2</sub>]. Also, they are very soluble in polar organic solvents.

[Me<sub>4</sub>N][Cd(S<sub>2</sub>CSC<sub>6</sub>H<sub>11</sub>)<sub>3</sub>] (2). A white suspension of 1' (1.063 g, 1.0 mmol) in 20 mL of CH<sub>2</sub>Cl<sub>2</sub> was treated with 10 mL of CS<sub>2</sub> until it became a bright yellow solution. Evaporation of the solvent or addition of ether afforded a yellow microcrystalline solid, which was filtered, washed in ether, and dried *in vacuo*. Yield: 1.367 g (90%). Calcd for C<sub>25</sub>H<sub>45</sub>-NCdS<sub>3</sub>: C, 39.48; H, 5.96; N, 1.84; S, 37.94. Found: C, 39.50; H, 6.05; N, 1.86; S, 37.70. This complex is soluble in most organic solvents.

**X-ray Crystallography.** [Et<sub>4</sub>N]<sub>2</sub>[Cd<sub>2</sub>(SC<sub>6</sub>H<sub>11</sub>)<sub>6</sub>] (1). Colorless cubic crystals were grown from a slowly evaporating acetonitrile solution. A suitable crystal was selected and mounted on a Philips PW-1100 four-circle diffractometer. Unit-cell parameters were determined from automatic centering of 25 reflections (4 ≤ θ ≤ 12) and refined by the least-squares method. Three reflections measured every 2 h as orientation and intensity control showed no significant decay during data collection. Lorentz-polarization corrections but no absorption corrections were made. The structure was solved by direct methods using the MULTAN system of computer programs<sup>14</sup> and refined by the full-matrix least-squares method using the SHELX-76 software package.<sup>15</sup> A carbon atom of the tetraethylammonium ion was located in a disordered position, assigning

(14) Main, P.; Fiske, S. E.; Hull, S. L.; Lessinger, L.; Germain, G.; Declercq, J. P.; Woolfson, M. M. *Multan 82, A System of Computer Programs for the Automatic Solution of Crystal Structures from X-ray Diffraction Data*; Universities of York and Louvain: York, England, and Louvain-la-Neuve, Belgium, 1982.

Table II. Selected Bond Distances (Å) and Angles (deg) for [Et<sub>4</sub>N]<sub>2</sub>[Cd<sub>2</sub>(SC<sub>6</sub>H<sub>11</sub>)<sub>6</sub>] (1)

Cd-S1	2.441(4)	Cd-S3	2.479(4)
Cd-S2	2.673(4)	Cd-S2'	2.606(4)
S1-Cd-S2	105.9(4)	S2-Cd-S3	112.6(4)
S1-Cd-S3	117.7(4)	S2-Cd-S2'	95.0(4)
S1-Cd-S2'	103.0(4)	S3-Cd-S2'	119.6(4)
Cd-S2-Cd'	85.0(4)		

an occupancy factor of 0.5 to each of the two positions according to the height of the difference Fourier. The positions of 30 H atoms were computed and refined with an overall isotropic temperature factor using a riding model, while the remaining nonhydrogen atoms were refined anisotropically. The final R factor was 0.065 (R<sub>w</sub> = 0.070) for all observed reflections. Data collection parameters are given in Table I. Main bond distances and angles are listed in Table II.

[Me<sub>4</sub>N][Cd(S<sub>2</sub>CSC<sub>6</sub>H<sub>11</sub>)<sub>3</sub>] (2). Yellow prismatic crystals were grown by vapor diffusion of ether into a methylene chloride solution containing some drops of CS<sub>2</sub>, and a suitable crystal was mounted on an Enraf-Nonius CAD4 diffractometer. Lattice parameters were obtained from least-squares refinement of 25 well-centered reflections. Standard reflections monitored every 200 measurements showed no significant decay. Lorentz-polarization corrections were applied. The absorption correction was made according to the empirical ψ-scan method<sup>16</sup> (minimum transmission 82.54, maximum 99.94, average 94.46). The structure was solved by direct methods using the SHELXS-86 program<sup>17</sup> and refined anisotropically by the least-squares method.<sup>15</sup> The atomic scattering factors were taken from the *International Tables for X-Ray Crystallography*.<sup>18</sup> The positions of all hydrogen atoms were calculated and refined with overall isotropic temperature factors (one for the cyclohexyl hydrogens and another for the methyl hydrogens). The final R factor was 0.043 (R<sub>w</sub> = 0.049) for all observed reflections. Computations were carried out on a DIGITAL VAX 8800 computer. Data collection parameters are listed in Table I. Selected bond lengths and angles are given in Table III.

(15) Sheldrick, G. M. *SHELX 76. A Computer Program for Crystal Structure Determination*; University of Cambridge: Cambridge, England, 1976.

(16) North, A. C. T.; Philips, D. C.; Mathews, F. S.; *Acta Crystallogr.* 1968, A24, 351.

(17) Sheldrick, G. M. *SHELXS-86. Crystallographic Computing 3*; Sheldrick, G. M., Krüger, C., Goddard, R., Eds.; Oxford University Press: England, 1985; pp 175–189.

(18) *International Tables for X-ray Crystallography*; Kynoch Press: Birmingham, England, 1974; Vol. 4, pp 99, 149.

**Table III.** Selected Bond Distances (Å) and Angles (deg) for  $[\text{Me}_4\text{N}][\text{Cd}(\text{SC}_6\text{H}_{11})_3]$  (2)

Cd-S11	2.714(2)	Cd-S12	2.722(2)
Cd-S21	2.680(2)	Cd-S22	2.697(2)
Cd-S31	2.667(2)	Cd-S32	2.717(2)

S11-Cd-S12	66.2(1)	S21-Cd-S22	66.5(1)	S31-Cd-S32	66.9(1)
S11-Cd-S22	156.2(1)	S12-Cd-S31	153.7(1)	S21-Cd-S32	160.0(1)
S11-Cd-S32	106.6(1)	S12-Cd-S22	103.1(1)	S21-Cd-S31	106.1(1)
S11-Cd-S31	98.8(1)	S12-Cd-S21	96.5(1)	S22-Cd-S31	98.3(1)
S11-Cd-S21	92.8(1)	S12-Cd-S32	95.7(1)	S22-Cd-S32	95.3(1)

**Table IV.** Tensor Principal Components<sup>a</sup> Corresponding to Different Environments of Cadmium. Isotropic Chemical Shift, Anisotropy, and Asymmetry Parameters Deduced from Principal Values

site (compd)	$\sigma_{11}$	$\sigma_{22}$	$\sigma_{33}$	$\sigma_{\text{iso}}^b = \frac{1}{3}(\sigma_{11} + \sigma_{22} + \sigma_{33})$	$\Delta\sigma^c$ anisotropy	$\eta^c$ asymmetry
CdS <sub>4</sub> (3)	712	699	514	+641(4)	-190	0.10
CdS <sub>4</sub> (1)	749	651	428	+610(20)	-273	0.54
CdS <sub>2</sub> Cl <sub>2</sub> (4)	640	595	425	+554(4)	-193	0.35
CdS <sub>2</sub> Br <sub>2</sub> (5)	617	562	345	+508(4)	-244	0.33
CdS <sub>2</sub> Br <sub>2</sub> (6)	668	536	224	+476(15)	-378	0.52
CdS <sub>2</sub> N <sub>2</sub> Br <sub>2</sub> (6)	665	603	11	+426(4)	-622	0.14
CdS <sub>2</sub> N <sub>2</sub> Cl (7)	584	499	149	+421(20)	-408	0.32
CdS <sub>2</sub> N <sub>2</sub> Cl <sub>2</sub> (7)	622	406	246	+425(3)	+295	0.81
CdS <sub>6</sub> (2)	356	107	68	+177(15)	+270	0.22

<sup>a</sup> In ppm referenced to 0.1 M aqueous  $\text{Cd}(\text{ClO}_4)_2$ . <sup>b</sup> Estimated errors are parenthesized as absolute values. <sup>c</sup> Parameters are defined according to ref 19c. For  $|\sigma_{11} - \sigma_{22}| < |\sigma_{22} - \sigma_{33}|$ ,  $\Delta\sigma = \sigma_{33} - \frac{1}{2}(\sigma_{11} + \sigma_{22})$  and  $\eta = (\sigma_{22} - \sigma_{11})/(\sigma_{33} - \sigma_{\text{iso}})$ ; for  $|\sigma_{11} - \sigma_{22}| > |\sigma_{22} - \sigma_{33}|$ ,  $\Delta\sigma = \sigma_{11} - \frac{1}{2}(\sigma_{33} + \sigma_{22})$  and  $\eta = (\sigma_{22} - \sigma_{33})/(\sigma_{11} - \sigma_{\text{iso}})$ . Absolute values of  $\Delta\sigma$  have been considered throughout the text.

**Solid-State NMR.**  $^{113}\text{Cd}$  CP MAS-NMR spectra were obtained at 295 K in a Bruker MSL-400 spectrometer, using a standard cross-polarization pulse sequence.<sup>19</sup> The external magnetic field was 9.4 T, and samples were spun at 4–4.5 kHz around an axis inclined  $54^\circ 44'$  with respect to this field. Spectrometer frequencies were set to 88.76 and 400.13 MHz for  $^{113}\text{Cd}$  and  $^1\text{H}$ , respectively. The Hartmann–Hahn condition<sup>19</sup> was obtained with the use of rotating  $H_1$  fields of 10.7 G for  $^1\text{H}$  and 48.1 G for  $^{113}\text{Cd}$ . For recorded spectra a contact time of 4 ms and a period between successive accumulations of 6–10 s were used. The amplifier bandwidth used was 60 kHz. The number of scans ranged from 500 to 5000 depending on the initial signal-to-noise ratio of each sample. Chemical shift values were referenced to 0.1 M  $\text{Cd}(\text{ClO}_4)_2$  aqueous solution.

The principal values of the shielding tensor were determined from the intensity of sidebands by using the moment analysis proposed by Maricq and Waugh.<sup>20</sup> In order to reduce experimental errors in intensity evaluation, base line correction by fourth-order polynomial fitting was performed. Special care was taken in considering the outer sidebands, whose intensity profiles were corrected by fitting them to Gaussian curves. Calculated isotropic chemical shift (Table IV) should coincide with the position of one of the sidebands. Thus, the difference between the calculated value and its closest sideband gives an estimate of the error in the determination of this parameter. Estimated errors for  $\sigma_{\text{iso}}$ , which range between 3 and 20 ppm in this study, are included in Table IV.

## Results

**X-ray Structures of Cadmium Complexes.** The synthesis and crystal structure of the complexes  $[\text{Cd}\{\mu\text{-SCH}(\text{CH}_2\text{CH}_2)_2\text{-NHMe}_2\}_2](\text{ClO}_4)_2 \cdot 2\text{H}_2\text{O}^{21}$  (3);  $[\text{CdX}_2\{\mu\text{-S}(\text{CH}_2)_3\text{NHMe}_2\}]$ ,  $\text{X} = \text{Cl}^{22}$  (4),  $\text{X} = \text{Br}^{23}$  (5);  $[\text{Cd}_4\{\text{S}(\text{CH}_2)_2\text{NMe}_2\}_4\text{Br}_4]$  (6); and  $[\text{Cd}_4\{\text{S}(\text{CH}_2)_2\text{NMe}_2\}_6\text{Cl}_2]$ <sup>24</sup> (7) have already been reported.

(19) (a) Hartmann, S. R.; Hahn, E. L. *J. Phys. Rev.* **1962**, *128*, 2042. (b) Pines, A.; Gibby, M. G.; Waugh, J. S. *J. Chem. Phys.* **1973**, *59*, 569. (c) Murphy, P. DuBois; Stevens, W. C.; Cheung, T. T. P.; Lacelle, S.; Gerstein, B. C.; Kurtz, D. M., Jr. *J. Am. Chem. Soc.* **1981**, *103*, 4400.

(20) Maricq, M. M.; Waugh, J. S. *J. Chem. Phys.* **1979**, *70*, 3300.

(21) Bayón, J. C.; Briand, M. C.; Briand, J. L.; González-Duarte, P. *Inorg. Chem.* **1979**, *18*, 3478.

(22) Casals, I.; González-Duarte, P.; Sola, J.; Font-Bardía, M.; Solans, J.; Solans, X. *J. Chem. Soc., Dalton Trans.* **1987**, 2391.

(23) Casals, I.; Clegg, W.; González-Duarte, P. *Acta Crystallogr.* **1993**, *C49*, 129.

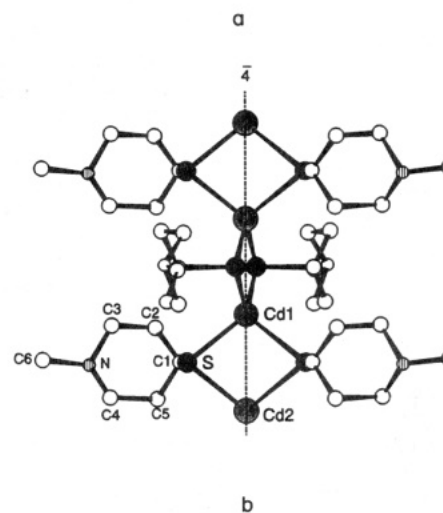
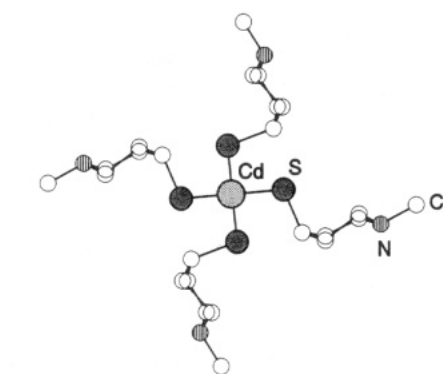
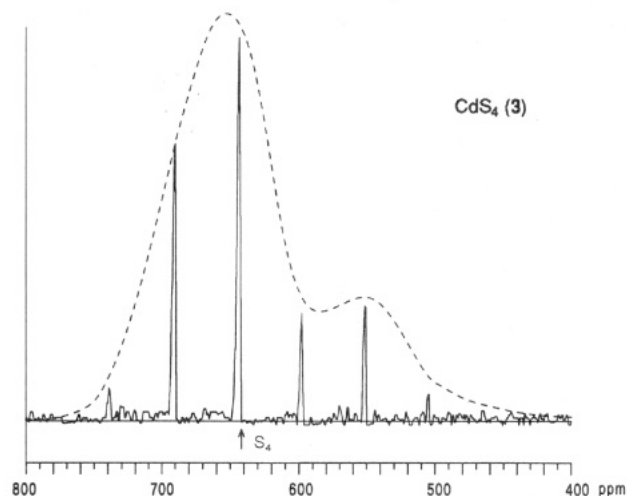


**Figure 1.**  $^{113}\text{Cd}$  CP/MAS-NMR spectrum of complex  $[\text{Cd}(\text{SC}_6\text{H}_9\text{NHMe}_2)_2][\text{ClO}_4]_2$  (3) and two views of its molecular structure: (a) down and (b) perpendicular to the 4-fold improper axis.

However, it seems convenient to give a brief description of each structure in order to facilitate the correlation between solid-state NMR parameters and structural data given in Tables IV and V, respectively.

The structure of 3 consists of infinite chains of cadmium atoms, each being tetrahedrally coordinated to four sulfur atoms. Each sulfur bridges two consecutive cadmium atoms, which are crystallographically independent and show a close coordination environment. A 4-fold improper rotation axis passes through cadmium atoms of the same chain (Figure 1). Complexes 4 and

(24) Casals, I.; González-Duarte, P.; Clegg, W.; Foces-Foces, C.; Hernández Cano, F.; Martínez Ripoll, M.; Gómez, M.; Solans, X. *J. Chem. Soc., Dalton Trans.* **1991**, 2511.

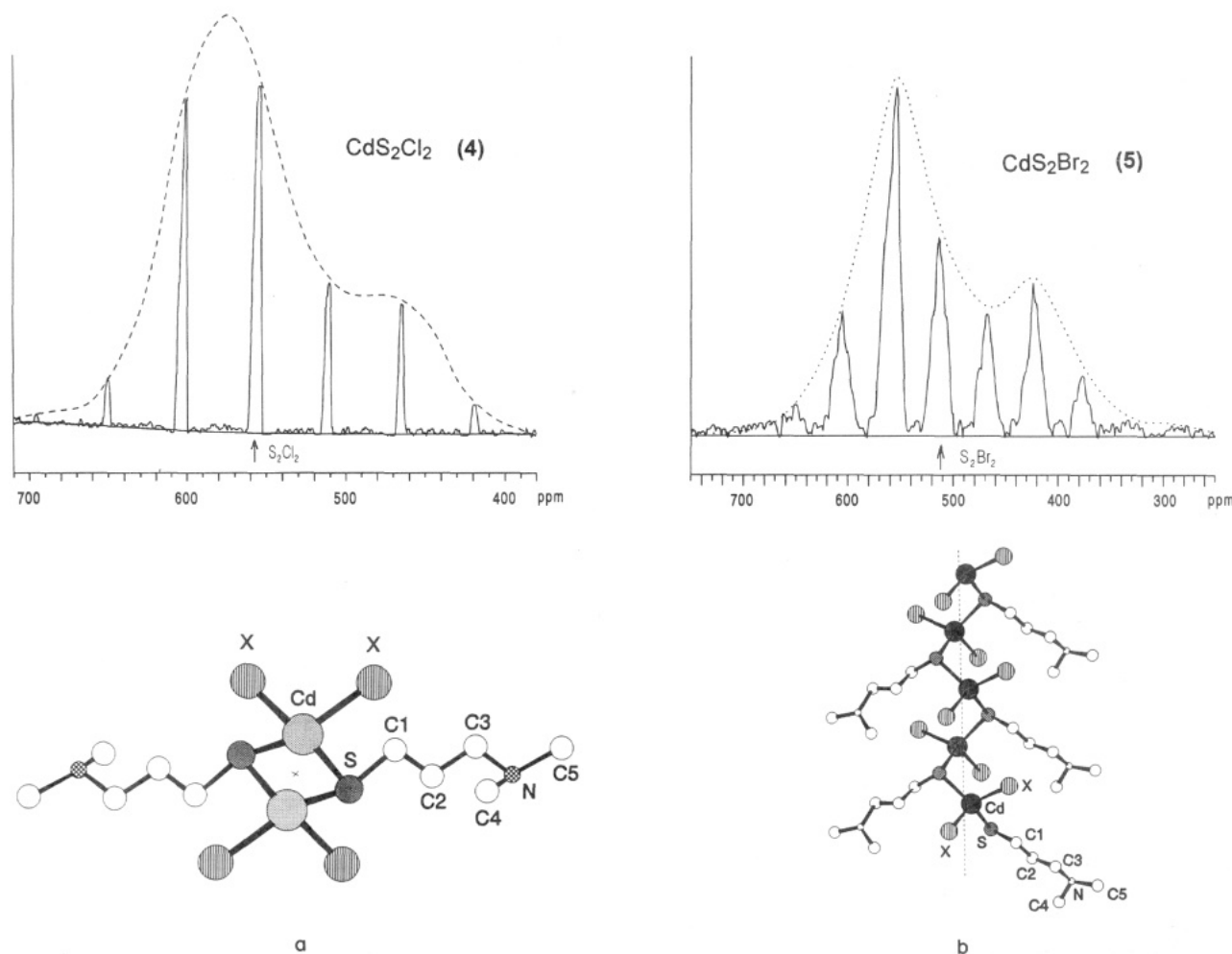


**Figure 2.**  $^{113}\text{Cd}$  CP/MAS-NMR spectra of isostructural complexes  $[\text{Cd}\{\text{S}(\text{CH}_2)_3\text{NHMe}_2\}\text{X}_2]$ ,  $\text{X} = \text{Cl}$  (4),  $\text{Br}$  (5), and two views of their molecular structure: (a) down and (b) perpendicular to the 2-fold helicoidal axis.

5 are isostructural and consist of polymeric chains of cadmium and sulfur atoms, as indicated in Figure 2. The latter bridge two consecutive symmetry-related cadmium atoms which complete coordination with either two chlorine (4) or two bromine (5) terminal atoms.

The structure of complexes 6 and 7, Figures 3 and 4, respectively, is formed by discrete centrosymmetric tetranuclear molecules with eight-membered rings of alternating metal and sulfur atoms. These  $\text{Cd}_4\text{S}_4$  rings have an extended-chair conformation with two opposite Cd atoms arranged on each side of the  $\text{Cd}'_2\text{S}_4$  plane. The two different cadmium coordination environments present in both 6 and 7 are described below.

The crystal structure of 1 consists of discrete dinuclear  $[\text{Cd}_2(\text{SC}_6\text{H}_{11})_6]^{2-}$  anions and  $[\text{NEt}_4]^+$  cations. The anion, whose  $\text{Cd}_2\text{S}_6$  core approaches a  $D_{2h}$  symmetry, Figure 5, can be described as two edge-sharing tetrahedra, each with a cadmium atom in their center. Thus, two sulfurs bridge the cadmium atoms, which complete coordination with two other sulfurs from terminal ligands. A crystallographic inversion center causes the  $\text{Cd}_2\text{S}_2$  unit to be exactly planar and cyclohexyl rings bonded to bridging sulfur atoms to adopt an *anti* configuration. Coordination around cadmium is somewhat distorted from that of a regular tetrahedron, as shown by bond distances and angles (Table II).

The structure of 2 consists of monomeric  $[\text{Cd}(\text{S}_2\text{CSC}_6\text{H}_{11})_3]^-$  anions and  $[\text{NMe}_4]^+$  cations. Equal numbers of *d* and *l* enantiomers of the anion are accommodated by the centrosymmetric lattice, which gives rise to only one crystallographically independent cadmium atom (Figure 6). The significant distortion from perfect octahedral symmetry toward a trigonal prism in the  $\text{CdS}_6$  core is essentially due to the constraints imposed by the

four-membered chelate rings, in which the S–Cd–S angles have been reduced from their normal values of  $90^\circ$  to  $66.5^\circ$  (mean value). Furthermore, the ideal angles of  $180^\circ$  in a regular octahedron range between  $153.7$  and  $159.9^\circ$  in the present structure. However, the opposite triangular faces determined by S11, S21, S31 and S12, S22, S32 are almost parallel (dihedral angle of  $6^\circ$ ) and show a twist angle of  $34^\circ$  with respect to the pseudo-3-fold axis. Thus, a  $D_3$  symmetry can be considered for the  $\text{CdS}_6$  core. Cd–S distances range between 2.668 and 2.721 Å and are the longest of all cadmium complexes here reported. This is the first example of a tris(thioxanthato)cadmium complex structurally characterized. Closely related species have been reported.<sup>25,26</sup>

**Solid-State NMR.**  $^{113}\text{Cd}$  CP/MAS-NMR spectra of complexes 1–7 are given in Figures 1–6 together with the structure of the corresponding solid complexes. Isotropic chemical shift values of different environments of cadmium are indicated with arrows at the bottom of each spectrum. In these spectra, envelopes of chemical shift patterns defined by each set of sidebands are represented to guide the eye, permitting a more rapid identification of the asymmetry of the shielding tensor. Principal elements deduced from sideband patterns are given in Table IV, where isotropic chemical shift, anisotropy, and asymmetry parameters corresponding to each site are also included.

The coordination environments and  $^{113}\text{Cd}$  CP/MAS spectra of two tetrahedrally coordinated cadmium complexes are shown

(25) Coucouvanis, D. *Prog. Inorg. Chem.* **1979**, 26, 301. Henkel, G.; Strasdeit, H.; Simon, W.; Krebs, B. *Inorg. Chim. Acta* **1983**, 76, L207.

(26) (a) Hoskins, B. F.; Kelly, B. P. *Inorg. Nucl. Chem. Lett.* **1972**, 8, 875. (b) Abrahams, B. F.; Hoskins, B. F.; Winter, G. *Inorg. Chim. Acta* **1988**, 150, 147.

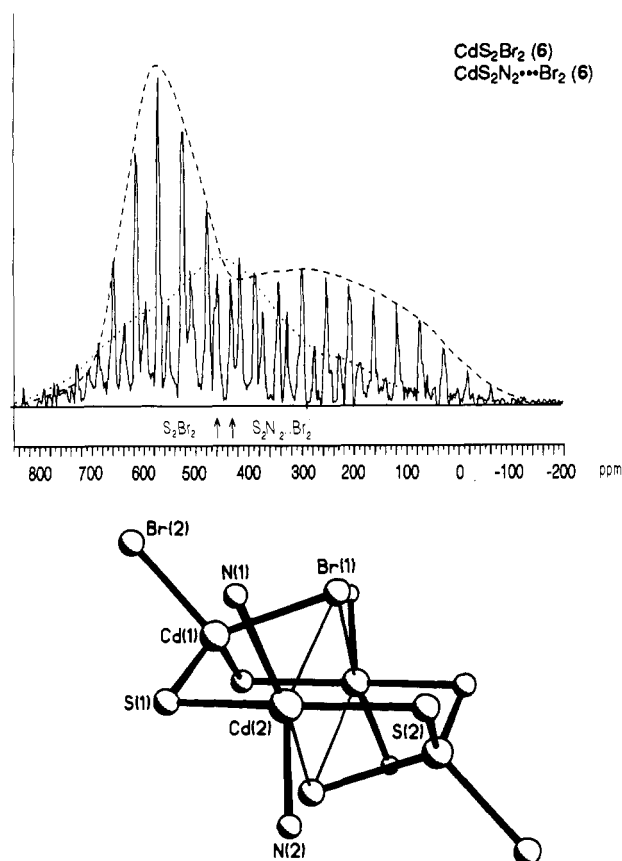


**Figure 3.**  $^{113}\text{Cd}$  CP/MAS-NMR spectrum of complex  $[\text{Cd}_4\{\text{S}(\text{CH}_2)_2\text{NMe}_2\}_4\text{Br}_4]$  (6) and corresponding molecular structure. Cd(2) distortion from tetrahedral toward octahedral coordination is shown by the following angles: S(1)–Cd(2)–S(2),  $161.0^\circ$ ; S(2)–Cd(2)–N(1),  $106.1^\circ$ ; S(2)–Cd(2)–N(2),  $83.4^\circ$ ; S(1)–Cd(1)–N(1),  $83.5^\circ$ ; S(1)–Cd(2)–N(2),  $106.6^\circ$ .

in Figures 1 and 5. All sulfur atoms in 3 (Figure 1) bridge consecutive Cd atoms, while in 1 (Figure 5) two sulfur atoms belong to terminal ligands and the other two to bridging ligands. As expected for species with a 4-fold improper axis,<sup>27</sup> the sideband pattern in the spectrum of 3 traces out the envelope of a shielding tensor with axial symmetry, which is almost ideal according to the value of  $\eta = 0.10$ . Although in 1 the corresponding envelope presents two maxima, the value of  $\eta = 0.54$  clearly indicates the existence of an orthorhombic distortion in agreement with the absence of any symmetry element on the cadmium atom. The anisotropy values for 3 and 1 correlate well with Cd–S bond distances and S–Cd–S angles. The four Cd–S bond lengths are practically equal in 3 but give rise to two pairs in 1. Furthermore, the angles around the cadmium atom resemble each other significantly more in the case of 3 than that of 1 (Table V). Consequently the anisotropy is smaller in the first case.

Polymeric complexes 4 and 5 contain  $\text{CdS}_2\text{X}_2$  centers, X = Cl (4) or Br (5). Coordination around cadmium is essentially tetrahedral in both cases but shows slightly more distortion in 5 than in 4. A view of the structure together with the  $^{113}\text{Cd}$  CP/MAS spectra is given in Figure 2. The sideband pattern in both spectra indicates a near-axial symmetry and correlates well with values calculated for  $\eta$ , 0.35 for 4 and 0.33 for 5, the proximity of these values agreeing with their isostructurality. Calculated values for the anisotropy, as indicated in Table IV, are very close to those found in 1 and 3 with  $\text{CdS}_4$  environments. However, this parameter is higher for 5,  $\Delta\sigma = 244$ , than for (4),  $\Delta\sigma = 193$ , which agrees with the fact that geometric parameters around cadmium in 4 are closer to those of a regular tetrahedron (Table V).

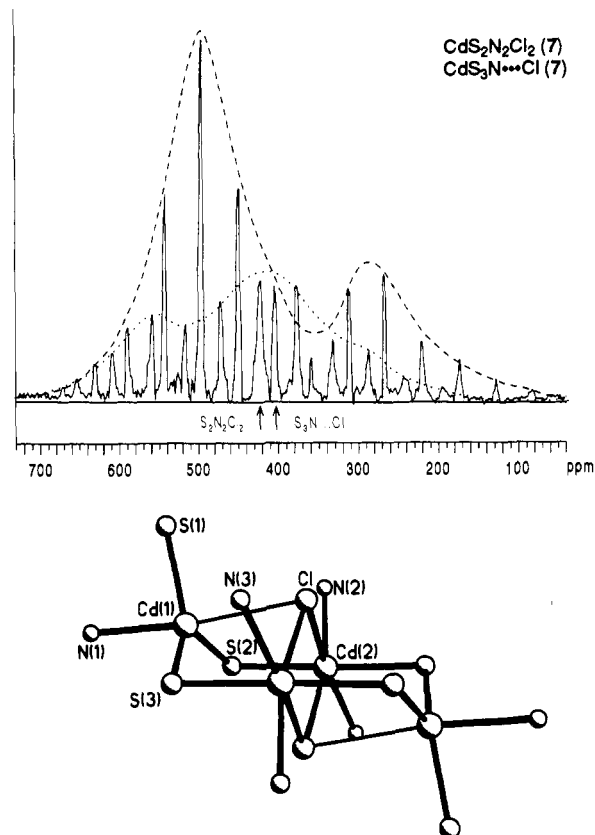


**Figure 4.**  $^{113}\text{Cd}$  CP/MAS-NMR spectrum of complex  $[\text{Cd}_4\{\text{S}(\text{CH}_2)_2\text{NMe}_2\}_6\text{Cl}_2]$  (7) and corresponding molecular structure. The planarity of the Cd(1) $\text{S}_3$  unit is shown by the following angles: S(1)–Cd(1)–S(2),  $118.4^\circ$ ; S(1)–Cd(1)–S(3),  $121.7^\circ$ ; S(2)–Cd(1)–S(3),  $119.1^\circ$ ;  $\Sigma(\text{S}–\text{Cd}–\text{S}) = 359.2^\circ$ . This plane is orthogonal to the N(1)–Cd(1) vector; average N(1)–Cd(1)–S angle =  $91^\circ$ .

Two different tetrahedral coordination environments are present in complex 6, whose structure and  $^{113}\text{Cd}$  CP/MAS spectrum are given in Figure 3. In this structure, two cadmium atoms are coordinated to two terminal bromine and two bridging sulfur atoms,  $\text{CdS}_2\text{Br}_2$ , with a distorted tetrahedral geometry, while the other two are also tetrahedrally coordinated to two bridging sulfur and two nitrogen atoms but with a severe distortion toward octahedral coordination,  $\text{CdS}_2\text{N}_2\cdots\text{Br}_2$ . The spectrum shows a pattern that can be decomposed into two families of sidebands having, respectively, isotropic chemical shifts of 476 and 426 ppm. This parameter lies between 365 and 390 ppm in tetrahedral  $\text{CdBr}_4^{2-}$  species.<sup>8,28</sup> No data have been reported so far for tetrahedral  $\text{CdN}_4$  sites, but we have estimated a range of 270–330 ppm for them using a linear method. These values show that bromine atoms induce a larger deshielding on cadmium than nitrogen atoms. Accordingly, isotropic chemical shifts of 476 and 426 ppm have been respectively assigned to  $\text{CdS}_2\text{Br}_2$  and  $\text{CdS}_2\text{N}_2$  centers, the former value being slightly lower than that obtained in 5 for the same environment. The shape of the envelope curve corresponding to  $\sigma_{\text{iso}} = 426$  ppm shows an axial symmetry, while that corresponding to  $\sigma_{\text{iso}} = 476$  reveals an orthorhombic distortion. This agrees with calculated  $\eta$  values of 0.14 and 0.52, respectively. Corresponding values for the anisotropy are high in both cases and suggest a large distortion from regular polyhedra, which seems to be particularly severe for the  $\text{CdS}_2\text{N}_2\cdots\text{Br}_2$  center (Table IV).

Substitution of two halogen atoms in 6 by additional aminoalkanthiolate ligands gives rise to 7, Figure 4, structurally related to its precursor. In this case two cadmium atoms are octahedrally coordinated to two bridging sulfur, two bridging

(27) Honkonen, R. S.; Ellis, P. D. *J. Am. Chem. Soc.* **1984**, *106*, 5488.

(28) Mennitt, P. G.; Shatlock, M. P.; Bartuska, V. J.; Maciel, G. E. *J. Phys. Chem.* **1981**, *85*, 2087.

Table V. Metrical Parameters in Cadmium-Sulfur Complexes<sup>a</sup>

compd	geometry around Cd	Cd-S, Å	Cd-N, Å	Cd-X, Å	Y-Cd-Z, deg	ref
[Cd(SC <sub>5</sub> H <sub>9</sub> NHMe) <sub>2</sub> ][ClO <sub>4</sub> ] <sub>2</sub> (3)	CdS <sub>4</sub> tetr	2.546(9), 2.550(9)			98.5(4), 115.2(4)	21
[Et <sub>4</sub> N] <sub>2</sub> [Cd <sub>2</sub> (SC <sub>6</sub> H <sub>11</sub> ) <sub>6</sub> ] (1)	CdS <sub>4</sub> tetr	2.441(4)–2.673(4)			95.0(4)–119.6(4)	this work
[Cd{S(CH <sub>2</sub> ) <sub>3</sub> NHMe <sub>2</sub> Cl <sub>2</sub> }] (4)	CdS <sub>2</sub> Cl <sub>2</sub> tetr	2.511(1), 2.516(1)		2.455(1), 2.507(1)	104.2(1)–120.3(1)	22
[Cd{S(CH <sub>2</sub> ) <sub>3</sub> NHMe <sub>2</sub> Br <sub>2</sub> }] (5)	CdS <sub>2</sub> Br <sub>2</sub> tetr	2.515(3), 2.516(3)		2.584(2), 2.640(2)	105.8(1)–127.0(1)	23
[Cd <sub>4</sub> {S(CH <sub>2</sub> ) <sub>2</sub> NMe <sub>2</sub> Br <sub>4</sub> }] (6)	CdS <sub>2</sub> Br <sub>2</sub> tetr	2.510(3), 2.518(3)		2.572(1), 2.681(2)	102.3(1)–126.3(1)	24
	CdS <sub>2</sub> N <sub>2</sub> ...Br <sub>2</sub> dist tetr <sup>b</sup>	2.501(2), 2.494(2)	2.366(9), 2.375(9)	3.295(2)–3.369(2)	83.4(2)–161.0(1) <sup>c</sup>	
[Cd <sub>4</sub> {S(CH <sub>2</sub> ) <sub>2</sub> NMe <sub>2</sub> Cl <sub>2</sub> }] (7)	CdS <sub>3</sub> N...Cl dist tetr <sup>d</sup>	2.464(2)–2.543(1)	2.507(5)	3.112(2)	83.4(1)–121.7(1) <sup>e</sup>	24
	CdS <sub>2</sub> N <sub>2</sub> Cl <sub>2</sub> oct	2.554(1), 2.559(1)	2.516(3), 2.558(3)	2.733(1), 2.735(1)	79.4(1)–103.8(1) <sup>f</sup>	
[Me <sub>4</sub> N][Cd(S <sub>2</sub> CSC <sub>6</sub> H <sub>11</sub> ) <sub>3</sub> ] (2)	CdS <sub>6</sub> pseudoct	2.668(2)–2.721(2)			164.6(1)–174.6(1) <sup>g</sup>	
					66.2(1)–106.6(1) <sup>h</sup>	this work
					153.7(1)–159.9(1) <sup>h</sup>	

<sup>a</sup> Where there are more than two values, the range is given. <sup>b</sup> Secondary interactions with two bromine atoms. <sup>c</sup> See Figure 4. <sup>d</sup> Secondary interaction with one chlorine atom. <sup>e</sup> See Figure 5. <sup>f</sup> 90° in a regular octahedron. <sup>g</sup> 180° in a regular octahedron.

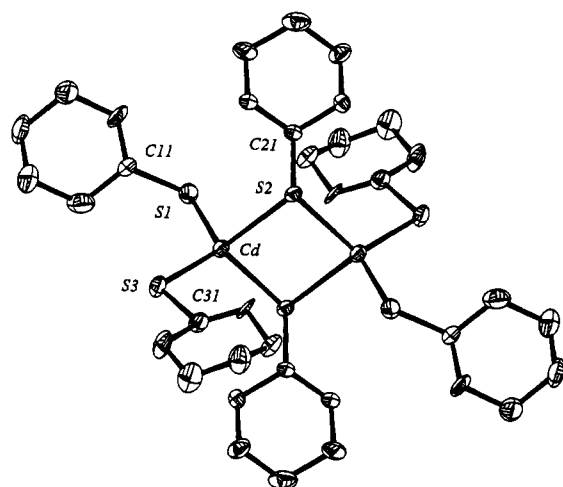
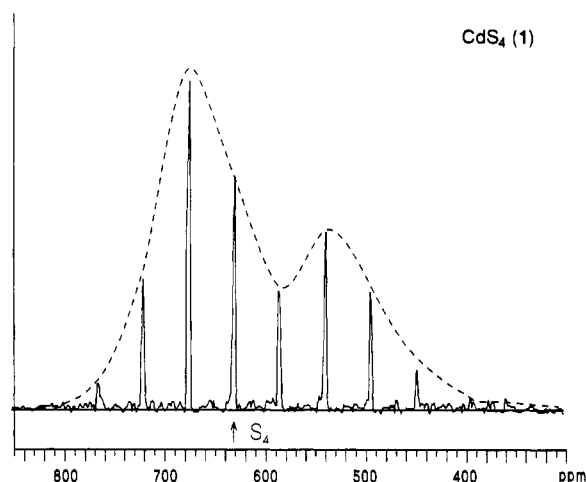


Figure 5. <sup>113</sup>Cd CP/MAS-NMR spectrum of complex [Et<sub>4</sub>N]<sub>2</sub>[Cd<sub>2</sub>(SC<sub>6</sub>H<sub>11</sub>)<sub>6</sub>] (1) and corresponding molecular structure.

chlorine, and two terminal nitrogen atoms, CdS<sub>2</sub>N<sub>2</sub>Cl<sub>2</sub>. The other two are bonded to two bridging sulfur atoms and to a chelating ligand to give a highly distorted CdS<sub>3</sub>N site, cadmium and all sulfur atoms being coplanar. A secondary interaction with a chlorine atom leads to a distorted trigonal-bipyramidal coordination, CdS<sub>3</sub>N...Cl. The <sup>113</sup>Cd CP/MAS spectrum of 7, Figure 4, like that of complex 6, shows two sets of sidebands. The isotropic chemical shifts at 421 and 425 ppm have been assigned to CdS<sub>3</sub>N...Cl and CdS<sub>2</sub>N<sub>2</sub>Cl<sub>2</sub> environments, respectively. The shape of the envelope curve corresponding to the former  $\sigma_{iso}$  shows a near-axial symmetry, while that of the latter is orthorhombically distorted. This is confirmed by the values of  $\eta$ , 0.32 and 0.81, respectively. Geometric features around cadmium at the CdS<sub>3</sub>N...Cl site support the axial symmetry found from NMR data and account for the previous assignments. The orthorhombic distortion of cadmium in the CdS<sub>2</sub>N<sub>2</sub>Cl<sub>2</sub> environment might be

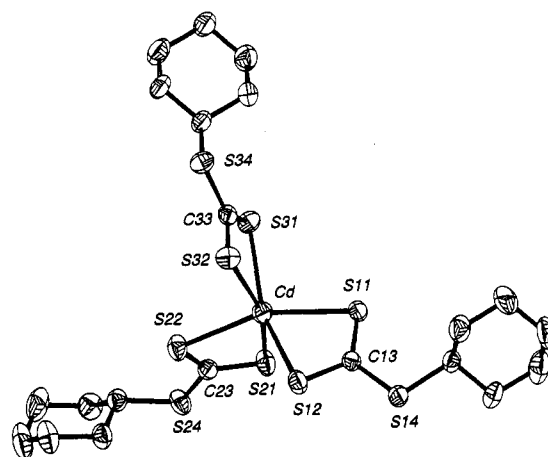
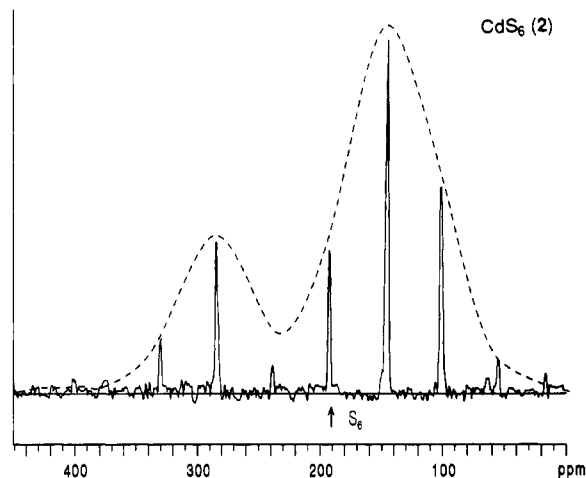


Figure 6. <sup>113</sup>Cd CP/MAS-NMR spectrum of complex [Me<sub>4</sub>N][Cd(S<sub>2</sub>CSC<sub>6</sub>H<sub>11</sub>)<sub>3</sub>] (2) and corresponding molecular structure.

attributed to the presence of three different donor atoms. Estimated values for  $\sigma_{iso}$  in octahedral CdS<sub>6</sub>, CdN<sub>6</sub>, and CdCl<sub>6</sub> centers<sup>7–11,28</sup> have allowed the calculation of a range of 420–430 ppm for CdS<sub>2</sub>N<sub>2</sub>Cl<sub>2</sub> by a linear method.

The structure of the tris(cyclohexylthioxanthato)cadmate(II) anion (2), Figure 6, consists of mononuclear units of cadmium octahedrally coordinated to sulfur atoms. As already indicated, despite the distortion from perfect octahedral symmetry, a pseudo-3-fold axis can be considered. The <sup>113</sup>Cd CP/MAS spectrum (Figure 6) indicates an axial symmetry around the cadmium nuclei, which is corroborated by the  $\eta$  value of 0.22. The isotropic chemical shift of Cd in the CdS<sub>6</sub> environment is the lowest of all cadmium centers reported here.

#### Discussion

On examining NMR parameters (Table IV) and crystallographic data (Table V) of solid cadmium complexes (1–7),



significant correlations can be found between shielding tensor parameters and the stereochemistry around the cadmium atom. However, the considerable number of experimental data requires an ordered analysis. Accordingly, the relationship between crystal or local symmetry around cadmium and the symmetry of the shielding tensor through  $\eta$  and  $\Delta\sigma$  parameters will be considered first.<sup>29</sup> This will be followed by a tentative orientation of the tensor in the molecular reference frame, which will be based on previous analyses of single-crystal oriented <sup>113</sup>Cd NMR studies in related complexes.<sup>4</sup> Additionally, trends observed in the variations of the individual tensor components of sites of close symmetry will be discussed in terms of structural features such as the dispersion of cadmium–ligand bond lengths and angles and the nature of the ligand.

**Relationship between Stereochemistry,  $\eta$ , and  $\Delta\sigma$ .** The asymmetry parameter,  $\eta$ , indicates axial symmetry for tetrahedral CdS<sub>4</sub> (3), distorted trigonal-bipyramidal CdS<sub>3</sub>N...Cl (7), and distorted trigonal-prismatic CdS<sub>6</sub> (2) centers. In the case of CdS<sub>4</sub> (3) the axial symmetry comes from the position of cadmium atoms on a  $\bar{4}$  ( $S_4$ ) axis in the unit cell.<sup>27</sup> An analogous situation occurs with CdS<sub>3</sub>N...Cl and CdS<sub>6</sub> sites, although only an idealized  $C_3$  axis passes through the cadmium atom, the local symmetry being close to  $C_{3v}$  and  $D_3$ , respectively. Even though  $\eta$  also indicates a near-axial symmetry for CdS<sub>2</sub>Cl<sub>2</sub> (4), CdS<sub>2</sub>Br<sub>2</sub> (5), and CdS<sub>2</sub>N<sub>2</sub>...Br<sub>2</sub> (6) sites, this symmetry is not observed in the crystal structure. A 2-fold axis passing through cadmium atoms could be idealized at CdS<sub>2</sub>Cl<sub>2</sub> (4) and CdS<sub>2</sub>Br<sub>2</sub> (5) sites. However, an axis of this order is not enough to justify an axially symmetric shielding tensor.<sup>5,7</sup> A possible explanation for the low value of  $\eta$  in CdS<sub>2</sub>N<sub>2</sub>...Br<sub>2</sub> (6) is given below. The orthorhombic distortion observed for CdS<sub>4</sub> (1), CdS<sub>2</sub>Br<sub>2</sub> (6), and CdS<sub>2</sub>N<sub>2</sub>Cl<sub>2</sub> (7) sites, particularly high in the latter, is in agreement with the absence at these metal centers of geometrical constraints due to the crystal symmetry.

As the anisotropy parameter,  $\Delta\sigma$ , is a measure of deviation from spherical symmetry, low values are expected for sites where distortion from cubic geometry is small.  $\Delta\sigma$  for CdS<sub>4</sub> (3), CdS<sub>4</sub> (1), CdS<sub>2</sub>Cl<sub>2</sub> (4), CdS<sub>2</sub>Br<sub>2</sub> (5), CdS<sub>2</sub>N<sub>2</sub>Cl<sub>2</sub> (7), and CdS<sub>6</sub> (2) environments ranges between 200 and 300 ppm. At the first four sites coordination around cadmium is close to a regular tetrahedron. In the last two it approaches that of an octahedron.

The different  $\Delta\sigma$  values for CdS<sub>2</sub>Cl<sub>2</sub> (4) and CdS<sub>2</sub>Br<sub>2</sub> (5), 193 and 244 ppm, respectively, correlate well with the geometric parameters around the cadmium atom. As indicated in Table V, bond lengths and angles involving cadmium are closer to each other in CdS<sub>2</sub>Cl<sub>2</sub> (range of distances, 2.45–2.52 Å; range of angles, 104–120°) than in CdS<sub>2</sub>Br<sub>2</sub> (corresponding ranges: 2.52–2.64 Å, 105–127°). A higher distortion in the coordination sphere of cadmium, particularly affecting bond distances, is found in the CdS<sub>2</sub>Br<sub>2</sub> site of complex 6. In this case the range in bond lengths (2.51–2.68 Å) is probably the cause for the high value of  $\Delta\sigma$  = 378. If we compare this coordination geometry and  $\Delta\sigma$  value with those of CdS<sub>2</sub>Br<sub>2</sub> (5), it can be concluded that relatively small differences in bond distances can induce a significant change in the anisotropy.

$\Delta\sigma$  values for CdS<sub>2</sub>N<sub>2</sub>...Br<sub>2</sub> (6) and CdS<sub>3</sub>N...Cl (7) sites are far from the range previously given. Distortion from tetrahedral toward octahedral coordination at the first site is particularly evidenced by the angles around cadmium: S–Cd–S 161.0(1)°; S–Cd–N<sub>av</sub> 95°. However, bromine–cadmium distances are long, averaging 3.34 Å (sum of the van der Waals radii for these atoms is estimated to be 3.5 Å<sup>30</sup>), and in fact the site is best described as tetrahedrally coordinated with two secondary bonding interactions [4 + 2]. The anisotropy parameter, 622 ppm, indicates that the actual geometry departs severely either from that of a tetrahedron (as in CdS<sub>4</sub> (3), CdS<sub>4</sub> (1), CdS<sub>2</sub>Cl<sub>2</sub> (4), and CdS<sub>2</sub>Br<sub>2</sub>

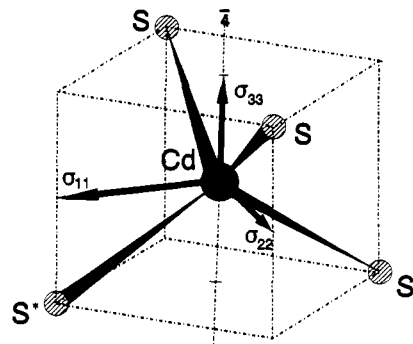


**Figure 7.** Proposed orientation of the shielding tensor in CdS<sub>4</sub> and CdS<sub>2</sub>X<sub>2</sub> (X = Cl, Br) environments. The  $S_4$  axis applies only to the CdS<sub>4</sub> (3) site. Sulfur atoms marked with an asterisk stand for bridging sulfurs in CdS<sub>4</sub> (1) and for terminal halogen atoms in CdS<sub>2</sub>X<sub>2</sub> (4–6) sites. In the three latter centers the orientation indicated in the figure is maintained for  $\sigma_{11}$ , while  $\sigma_{22}$  and  $\sigma_{33}$  are interchanged.

(5)) or from that of an octahedron (CdS<sub>2</sub>N<sub>2</sub>Cl<sub>2</sub> (7)), where  $\Delta\sigma$  has a significantly lower value. The fact that coordination around Cd at the CdS<sub>3</sub>N...Cl (7) site is distorted trigonal-bipyramidal with a long Cd–Cl distance of 3.11 Å, [4 + 1], is in accordance with a  $\Delta\sigma$  value out of the 200–300-ppm range.

**Tensor Element–Structure Correlations.** The individual components of the shielding tensor give reliable information about perturbations of cadmium closed-shell configuration at a given metal site.<sup>12</sup> However, in order to relate tensor elements with structural features about the metal center, we need to know the orientation of the shielding tensor in the molecular frame. This is accomplished by means of single-crystal oriented NMR experiments or, only qualitatively, in solid complexes of known structure by using the empirical rules developed by Ellis.<sup>7,27,31</sup> In this section the possible orientation of distinct <sup>113</sup>Cd shielding tensors occupying a variety of site symmetries will be analyzed. Variations in tensor principal components caused by changes in the geometry and nature of donor atoms will also be discussed.

**CdS<sub>2</sub>X<sub>2</sub> (X = S, Cl, Br) Sites in Complexes 1 and 3–6.** Shielding tensor principal axes corresponding to CdS<sub>4</sub> (3) and CdS<sub>4</sub> (1) have been oriented (Figure 7) following the precepts laid down by Ellis,<sup>31</sup> already verified in CdS<sub>2</sub>N<sub>2</sub> sites.<sup>4</sup> These establish that a tensor element reflects its orthogonal environment as the shielding effects of a given M–L bond are maximal at orthogonal directions to the M–L vector and decrease at directions forming lower angles. The fact that the four Cd–S distances in the CdS<sub>4</sub> (3) site are almost equal accounts well for the proximity of  $\sigma_{11}$  and  $\sigma_{22}$  values. When the coordination tetrahedron in Figure 7 represents the CdS<sub>4</sub> (1) site, two Cd–S distances decrease and the other two increase with respect to CdS<sub>4</sub> (3). Then, according to the assumed orientation,  $\sigma_{11}$  shifts downfield whereas  $\sigma_{22}$  moves in the opposite direction. Substitution of the two bridging sulfur atoms in CdS<sub>4</sub> sites by two halogen atoms, which are more shielding than the former, causes  $\sigma_{22}$  to shift upfield and, hence, to become  $\sigma_{33}$ . Comparing isostructural complexes containing CdS<sub>2</sub>Cl<sub>2</sub> (4) and CdS<sub>2</sub>Br<sub>2</sub> (5) sites, it is evident that  $\sigma_{11}$  has a similar value in both sites, which agrees with the practically equal Cd–S distances. On the other hand, the different nature of halogen atoms, bromine being more shielding than chlorine, determines the lower value of  $\sigma_{33}$  observed in CdS<sub>2</sub>Br<sub>2</sub> (5). However, the great similarity of cadmium environments in both CdS<sub>2</sub>Br<sub>2</sub> sites, complexes 5 and 6, is not evidenced by the corresponding elements of the tensor.

Variations in shielding tensor components of different sites are not necessarily reflected in the isotropic chemical shift, since upfield shift in one element may be canceled by opposing effects

(29) Mason, J., Ed. *Multinuclear NMR*; Plenum Press: New York, 1987.

(30) Hueheey, J. E. *Inorganic Chemistry*, 3rd ed.; Harper and Row: New York, 1983, pp 258–259.

(31) Ellis, P. D. *The Multinuclear Approach to NMR Spectroscopy*; Lambert, J. B., Ridell, F. G., Eds.; D. Reidel: Dordrecht, The Netherlands, 1983; Chapter 22.

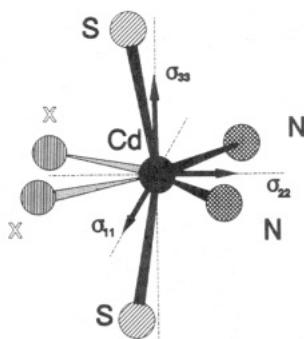


**Figure 8.** Proposed orientation of the shielding tensor in  $\text{CdS}_2\text{N}_2\cdots\text{Br}_2$  (6) and  $\text{CdS}_2\text{N}_2\text{Cl}_2$  (7) sites.  $\sigma_{11}$  and  $\sigma_{22}$  can be considered coplanar with both Cd-N bonds, the former element being perpendicular to the plane of the paper and the latter bisecting the X-Cd-X and N-Cd-N angles.  $\sigma_{33}$  is approximately collinear with both Cd-S bonds. Long-range interactions with bromine atoms in the  $\text{CdS}_2\text{N}_2\cdots\text{Br}_2$  (X = Br) site become bonding in  $\text{CdS}_2\text{N}_2\text{Cl}_2$  (X = Cl). Angles formed by Cd-ligand vectors and tensor principal axes in 7 are Cd-Cl vector- $\sigma_{11}$ , 50°; Cd-N vector- $\sigma_{11}$ , 38°; Cd-Cl vector- $\sigma_{22}$ , 41°; Cd-N vector- $\sigma_{22}$ , 52°. In 6: Cd-N vector- $\sigma_{11}$ , 32°; Cd-N vector- $\sigma_{22}$ , 58°; Cd-Br vector- $\sigma_{11}$ , 55°; Cd-Br vector- $\sigma_{22}$ , 37°.

of the other elements. However, a fairly good correlation is found between  $\sigma_{\text{iso}}$  and the nature of donor atoms in tetrahedrally coordinated species. According to Table IV,  $\sigma_{\text{iso}}$  decreases as sulfur atoms in  $\text{CdS}_4$  sites are subsequently substituted by chlorine or bromine. The last sequence still holds if nitrogen is included, although the  $\text{CdS}_2\text{N}_2\cdots\text{Br}_2$  (6) site shows a significant distortion from tetrahedral coordination. The coincidence of  $\sigma_{\text{iso}}$  corresponding to this site with that of  $\text{CdS}_2\text{N}_2\text{Cl}_2$  (7) finds an explanation through the analysis of the individual elements of the respective shielding tensors. We also note that  $\sigma_{\text{iso}}$  corresponding to the  $\text{CdS}_3\text{N}\cdots\text{Cl}$  (7) site might be expected to have a somewhat higher value considering that only one sulfur in a  $\text{CdS}_4$  site has been replaced by a nitrogen atom. The pronounced distortion in the geometry around cadmium, the  $\text{CdS}_3$  fragment being on a plane, may influence its  $\sigma_{\text{iso}}$  value.

**$\text{CdS}_2\text{N}_2\cdots\text{Br}_2$  (6) and  $\text{CdS}_2\text{N}_2\text{Cl}_2$  (7) Sites.** The directions of the three tensor principal axes, Figure 8, have been selected according to previous results based on solid-state NMR studies on a tetrahedral  $[\text{Cd}(\text{SR})_2(\text{N-donor})_2]$  site<sup>4</sup> and a digonal  $[\text{Hg}(\text{SR})_2]$ <sup>5</sup> complex. The former possesses a distorted cadmium center, and the latter has an almost linear metal-sulfur coordination, both features also present in the  $\text{CdS}_2\text{N}_2\cdots\text{Br}_2$  (6) site. For the presumed orientation, the values of  $\sigma_{11}$  and  $\sigma_{22}$  tensor elements should be highly downfield shifted, as they would reflect the well-known deshielding effect of sulfur atoms. In contrast, the  $\sigma_{33}$  element, which is almost collinear with both cadmium-sulfur bonds, would be the least deshielded, the large upfield shift observed reflecting the shielding contributions of its orthogonal environment. These would arise from the cadmium-nitrogen bonds and especially from the bromine atoms, as their distance to the cadmium is only slightly below the sum of the van der Waals radii.<sup>30</sup> In addition to the major deshielding influences of the cadmium-sulfur bonds, both orthogonal to  $\sigma_{11}$  but forming an angle of 80° with  $\sigma_{22}$ , in-plane shielding effects of Cd-N bonds and secondary interactions also affect  $\sigma_{11}$  and  $\sigma_{22}$ , although substantially less than  $\sigma_{33}$  because of their relative position with respect to Cd-N and Cd-Br vectors. On the assumption that the  $\sigma_{22}$  principal axis bisects the angle formed by the two Cd-N vectors, these would be at a greater angle from  $\sigma_{22}$  than from  $\sigma_{11}$ , and thus the former would be more influenced than the latter by the deshielding effect of nitrogen atoms. Conversely,  $\sigma_{11}$  would be somewhat more affected than  $\sigma_{22}$  by Cd-Br interactions, although this minor contribution is less deshielding. The overall effect of the shielding influences of sulfur, nitrogen, and bromine atoms would account for the close values of  $\sigma_{11}$  and  $\sigma_{22}$ . Therefore, the similarity between these two elements, together with their

expected great difference with respect to  $\sigma_{33}$ , would explain both the large anisotropy and the axial symmetry of the shielding tensor found experimentally.

The orientation assigned to tensor elements at the  $\text{CdS}_2\text{N}_2\cdots\text{Br}_2$  (6) site can also be applied to  $\text{CdS}_2\text{N}_2\text{Cl}_2$  (8) (Figure 8). The main difference with the previous site is that chlorine atoms belong to the first coordination sphere of the metal center. Accordingly,  $\sigma_{11}$ , more affected by their deshielding contribution, separates from  $\sigma_{22}$ . As a consequence, the relation  $\sigma_{11} > \sigma_{22} > \sigma_{33}$  should apply, which is fully borne out by the values found for the shielding tensor components.

Distortions in ligand geometry can give rise to significant variations in the values of tensor elements. Thus, by comparing geometric parameters around Cd, it is possible to explain the different evolution of  $\sigma_{11}$  and  $\sigma_{22}$  on passing from  $\text{CdS}_2\text{N}_2\cdots\text{Br}_2$  (6) to  $\text{CdS}_2\text{N}_2\text{Cl}_2$  (7) sites. On the basis of the smaller Cd-S distance in (6), 0.06 Å shorter, a greater deshielding would be expected for the corresponding in-plane tensor components  $\sigma_{11}$  and  $\sigma_{22}$ . Values in Table IV confirm this expectation. Two other changes in bond distances have to be considered. The lengthening of the Cd-N distance (0.17 Å) in  $\text{CdS}_2\text{N}_2\text{Cl}_2$  (7) increases the tendency of  $\sigma_{22}$  to shift upfield, while  $\sigma_{11}$  tends to displace in the opposite direction because of the shortening of the Cd-halogen distance. These in-plane interactions may contribute to separate  $\sigma_{11}$  and  $\sigma_{22}$  values, and as a result, the axiality of the tensor in 6 is broken and an orthorhombic distortion appears in 7. The same interactions also affect the out-of-plane tensor element  $\sigma_{33}$ , the drastic reduction of the Cd-X distance in 7 being the dominant contribution to its significant downfield displacement. Although the stereochemistry of the two sites is different, the increase of  $\sigma_{33}$  compensates for the lowering of  $\sigma_{11}$  and  $\sigma_{22}$  and the average of the three principal elements,  $\sigma_{\text{iso}}$ , remains unaffected within the experimental error.

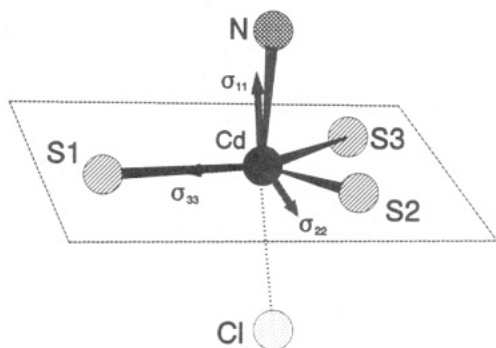
NMR data corresponding to the  $\text{CdS}_2\text{N}_2\cdots\text{Br}_2$  (6) site can be compared with literature values for other cadmium complexes containing  $\text{CdS}_2\text{N}_2$  centers (Table VI), already studied by solid-state NMR.<sup>4</sup> Geometric parameters around cadmium in  $\text{CdS}_2\text{N}_2\cdots\text{Br}_2$  (6) and  $\text{CdS}_2\text{N}_2$  (8) show a significant distortion from ideal tetrahedral coordination. If assuming that the overall angular distortions could be considered comparable, thus affecting the corresponding  $\Delta\sigma$  value similarly, the fact that this parameter is somewhat larger for the site 8 may find an explanation through bond distances. It has already been indicated that small differences such as 0.03 Å may induce significant variations in tensor principal components.<sup>10</sup> Accordingly the somewhat shorter Cd-N distance and the significantly shorter Cd-S bond length in site 8 would cause downfield shifts of  $\sigma_{33}$  and  $\sigma_{11}$ , respectively. Assuming that  $\Delta\sigma$  corresponds roughly to the separation between  $\sigma_{33}$  and  $\sigma_{11}$  components and taking into account that the displacement of  $\sigma_{11}$  is greater than that of  $\sigma_{33}$ , the net effect is an increase in  $\Delta\sigma$ .

A different situation arises when comparing  $\text{CdS}_2\text{N}_2\cdots\text{Br}_2$  (6) with  $\text{CdS}_2\text{N}_2$  in 9 and 10 because the overall angular distortions in the three sites are not comparable but significantly smaller in the last two cases. Accordingly, a smaller  $\Delta\sigma$  value would be expected for 9 and 10, which agrees with the experimental values given in Table VI. Moreover, differences in bond distances in the  $\text{CdS}_2\text{N}_2\cdots\text{Br}_2$  (6) and  $\text{CdS}_2\text{N}_2$  (9) sites affect  $\Delta\sigma$  in the same direction as the angular distortion. Thus, the shorter Cd-S distance in 9 compared to  $\text{CdS}_2\text{N}_2\cdots\text{Br}_2$  (6) causes  $\sigma_{11}$  to be greater in the former site. A similar but enhanced effect is observed in the  $\sigma_{33}$  value, probably due to the significantly shorter Cd-N distance in site 9. As a consequence  $\Delta\sigma$  is smaller in this site. Although the overall effects of the changes in the sulfur and nitrogen bond distances almost cancel and give very close isotropic chemical shifts in 8-10,<sup>4</sup> a lower value is found for  $\text{CdS}_2\text{N}_2\cdots\text{Br}_2$  (6), which agrees well with the fact that Cd-N and Cd-S distances are the longest of all the  $\text{CdS}_2\text{N}_2$  sites considered.

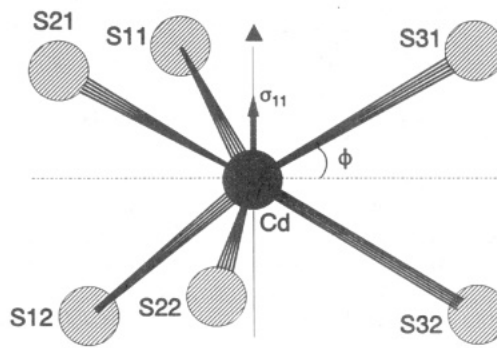


**Table VI.** Structural and  $^{113}\text{Cd}$  NMR Data for Complexes Containing a  $\text{CdS}_2\text{N}_2$  Site

site (complex)	geom params (av values), Å, deg	shielding tensor components, ppm	$\Delta\sigma$	$\sigma_{\text{iso}}$	ref
$\text{CdS}_2\text{N}_2\cdots\text{Br}_2$ (6)	$d(\text{Cd-S}) = 2.495$ $d(\text{Cd-N}) = 2.37$ $\text{S-Cd-S} = 161$ $\text{N-Cd-N} = 116$ $\text{N-Cd-S} = 95$	$\sigma_{11} = 665$ $\sigma_{22} = 603$ $\sigma_{33} = 11$	622	426	this work
$\text{CdS}_2\text{N}_2$ (8)	$d(\text{Cd-S}) = 2.43$ $d(\text{Cd-N}) = 2.34$ $\text{S-Cd-S} = 126$ $\text{N-Cd-N} = 70$ $\text{N-Cd-S} = 112$	$\sigma_{11} = 815$ $\sigma_{22} = 630$ $\sigma_{33} = 31$	691	492	4
$\text{CdS}_2\text{N}_2$ (9)	$d(\text{Cd-S}) = 2.46$ $d(\text{Cd-N}) = 2.26$ $\text{S-Cd-S} = 126$ $\text{N-Cd-N} = 94$ $\text{N-Cd-S} = 108$	$\sigma_{11} = 790$ $\sigma_{22} = 528$ $\sigma_{33} = 135$	523	484	4
$\text{CdS}_2\text{N}_2$ (10)	likely to be quite similar to $\text{CdS}_2\text{N}_2$ (9)	$\sigma_{11} = 760$ $\sigma_{22} = 530$ $\sigma_{33} = 183$	463	492	4

**Figure 9.** Proposed orientation of the shielding tensor in the  $\text{CdS}_3\text{N}\cdots\text{Cl}$  (7) site.  $\sigma_{11}$  is orthogonal to the  $\text{CdS}_3$  plane, and  $\sigma_{33}$  is collinear with the shortest cadmium-sulfur bond ( $\text{Cd-S}_1$ ,  $\text{Cd-S}_2$ , and  $\text{Cd-S}_3$  distances are 2.46, 2.54, and 2.53 Å, respectively).

**$\text{CdS}_3\text{N}\cdots\text{Cl}$  (7) Site.** On examining the shielding tensor components corresponding to the  $\text{CdS}_3\text{N}\cdots\text{Cl}$  (7) site, an axial symmetry is revealed with  $\sigma_{33}$  as the unique axis of the tensor ( $\sigma_{11} \approx \sigma_{22} > \sigma_{33}$ ). The coplanarity of cadmium and sulfur atoms at this site allows us to compare it with the geometry found in  $[\text{Ph}_4\text{P}][\text{Cd}(\text{S-2,4,6-}i\text{-Pr}_3\text{C}_6\text{H}_2)_3]$ ,<sup>5</sup> which has a  $C_{3h}$  symmetry and also shows axial distortion in its shielding tensor. However, in the latter the unique axis is  $\sigma_{11}$  with tensor elements varying in the sequence  $\sigma_{11} > \sigma_{22} \approx \sigma_{33}$ , in good agreement with the symmetry around the cadmium atom. Even though each of the three  $\text{S-Cd-S}$  angles in  $\text{CdS}_3\text{N}\cdots\text{Cl}$  (7) is within a few degrees of  $120^\circ$ , one  $\text{Cd-S}$  distance departs significantly from the other two, thus approaching a Y-shaped geometry,  $C_s$  symmetry, rather than the  $C_{3v}$  previously considered. Consequently, it seems more appropriate to compare  $\text{CdS}_3\text{N}\cdots\text{Cl}$  (7) with a Y-shaped isomer of the previous  $[\text{Cd}(\text{S-2,4,6-}i\text{-Pr}_3\text{C}_6\text{H}_2)_3]$  anion, which shows an average cadmium-sulfur distance of 2.43 Å.<sup>5</sup> As expected for this geometry, the principal axes of the shielding tensor depart from ideal axiality ( $\sigma_{11} = 939$ ,  $\sigma_{22} = 540$ ,  $\sigma_{33} = 360$ ;  $\eta = 0.55$ ). However,  $\sigma_{11}$ ,  $\sigma_{22}$ , and  $\sigma_{33}$  values for  $\text{CdS}_3\text{N}\cdots\text{Cl}$  (7) differ substantially from the previous values probably because of the presence of the nitrogen and chlorine atoms and the longer  $\text{Cd-S}$  distances (average 2.51 Å). One may rationalize the behavior of the tensor assuming that its principal axes are oriented relative to cadmium-ligand bonds, as indicated in Figure 9. As shown there,  $\sigma_{11}$  is perpendicular to the  $\text{CdS}_3$  plane and, hence, would be deshielded by all three sulfur atoms. As  $\sigma_{33}$  is collinear with the shortest cadmium-sulfur bond, both  $\sigma_{33}$  and  $\sigma_{22}$  would be deshielded by nitrogen and chlorine atoms but only the latter additionally affected by a short  $\text{Cd-S}$  bond at a  $90^\circ$  angle. Thus, the overall

**Figure 10.** Proposed orientation of the unique axis in the  $\text{CdS}_6$  (2) site, which is collinear with the idealized 3-fold rotation axis.

effect of these interactions would lead to the relation  $\sigma_{11} > \sigma_{22} > \sigma_{33}$ , which is relatively close to that found.

**$\text{CdS}_6$  (2) Site.** Two NMR parameters corresponding to the  $\text{CdS}_6$  (2) site deserve a special comment: the value of  $\sigma_{11}$ , the unique axis, and the extremely low value found for the isotropic shift. It is well-known that in trigonal-planar complexes, the most deshielded tensor component coincides with the unique element, since the 3-fold axis is perpendicular to the metal-ligand vectors in this geometry.<sup>5</sup> The same assessment should hold for the  $\text{CdS}_6$  (2) site with  $D_3$  symmetry (Figure 10). However, in this case cadmium-sulfur vectors are not coplanar but form an average angle with a plane normal to a  $C_3$  axis of  $28.8^\circ$ . Thus, their overall deshielding effect along the direction of  $\sigma_{11}$  must be comparatively lower.

The value of  $\sigma_{\text{iso}}$ , 177 ppm, is among the lowest found for cadmium complexes with sulfur-containing ligands, except for one cadmium-thiourea species with a  $\text{CdS}_2\text{O}_2\cdots\text{O}_2$  site, where the great shielding observed,  $\sigma_{\text{iso}} = 98$  ppm, is not due to sulfur atoms.<sup>12</sup> Cadmium complexes with *gem*-dithio ligands show lower values for  $\sigma_{\text{iso}}$ , as indicated in Table VII, than those with unidentate thiolates, these ranging between 600 and 700 ppm.<sup>8</sup> The isotropic shift for the  $\text{CdS}_6$  (2) site (177 ppm) correlates well with that observed in solution for the four tris(dithio) complexes given in Table VII (range 177–277 ppm), the crystal structure of two of them being very close to that of 2. It seems likely that  $\sigma_{\text{iso}}$  values reported in this table are partially due to the cadmium-sulfur distances found in all these complexes, which are significantly longer than those in comparable cadmium-thiolates.<sup>32</sup> In fact

(32) Dance, I. G. *Polyhedron* **1986**, 5, 1037.(33) Rietveld, H. M.; Maslen, E. N. *Acta Crystallogr.* **1965**, 18, 429.(34) Iimura, Y.; Ito, T.; Hagihara, H. *Acta Crystallogr., Sect. B* **1972**, 28, 2271.(35) Khan, O. F. Z.; O'Brien, P. *Polyhedron* **1991**, 10, 325.

**Table VII.** <sup>113</sup>Cd NMR Data and Coordination Geometry for [Cd(SS)<sub>2</sub>] and [Cd(SS)<sub>3</sub>]<sup>-2-</sup> Complexes

complex	$\sigma_{\text{iso}}^a$	$\delta(\text{solv, temp}^b)^a$	coord geom	$d(\text{Cd-S}), \text{\AA}$	ref
[Cd(S <sub>2</sub> CO- <i>n</i> -Bu) <sub>2</sub> ]	445		CdS <sub>4</sub> tetr	2.56–2.62	28, 33
[Cd(S <sub>2</sub> COEt) <sub>2</sub> ]	414		CdS <sub>4</sub> tetr	2.54–2.59	28, 34
[Cd(S <sub>2</sub> CNEt <sub>2</sub> ) <sub>2</sub> ]	377		CdS <sub>5</sub> tetrag pyr–trig bipy	2.80; 2.54–2.64	28, 35, 36
[Cd( <i>i</i> -MNT) <sub>2</sub> ] <sup>2-</sup> <sup>c</sup>	258		CdS <sub>4</sub> sq pl	2.59, 2.68	37
[Cd(S <sub>2</sub> CSC <sub>6</sub> H <sub>11</sub> ) <sub>3</sub> ] <sup>-</sup> (2)	177		CdS <sub>6</sub> trig prism–oct	2.67–2.72	this work
[Cd(S <sub>2</sub> COEt) <sub>3</sub> ] <sup>-</sup>		277 (CHCl <sub>3</sub> )	CdS <sub>5</sub> tetrag pyr	2.51; 2.65–2.72	9, 26a
[Cd(S <sub>2</sub> CNEt <sub>2</sub> ) <sub>3</sub> ] <sup>-</sup>		177 (CH <sub>2</sub> Cl <sub>2</sub> , –95 °C)	CdS <sub>6</sub> trig prism–oct	2.66–2.75	38, 39
[Cd(S <sub>2</sub> CO- <i>i</i> -Pr) <sub>3</sub> ] <sup>-</sup>		238 (CH <sub>2</sub> Cl <sub>2</sub> , –90 °C)			38
[Cd(S <sub>2</sub> P(O- <i>i</i> -Pr) <sub>3</sub> ) <sub>3</sub> ] <sup>-</sup>		196 (CH <sub>2</sub> Cl <sub>2</sub> , –95 °C)	CdS <sub>6</sub> trig prism–oct	2.66–2.78	38, 39
[Cd(S <sub>2</sub> P(O- <i>i</i> -Pr) <sub>2</sub> ) <sub>2</sub> ]		380 (CH <sub>2</sub> Cl <sub>2</sub> , –90 °C)	CdS <sub>4</sub> tetr	2.49–2.59	38, 40, 41
[Cd(S <sub>2</sub> P(OC <sub>6</sub> H <sub>11</sub> ) <sub>2</sub> ) <sub>2</sub> ]		377 (CH <sub>2</sub> Cl <sub>2</sub> )			40
[Cd(S <sub>2</sub> P(O- <i>n</i> -Bu) <sub>2</sub> ) <sub>2</sub> ]		353 (CH <sub>2</sub> Cl <sub>2</sub> )			40
[Cd(S <sub>2</sub> CN( <i>n</i> -Bu) <sub>2</sub> ) <sub>2</sub> ]		325 (CHCl <sub>3</sub> )	CdS <sub>5</sub> tetrag pyr–trig bipy	2.89; 2.51–2.60	42
[Cd(S <sub>2</sub> CNR <sub>1</sub> R <sub>2</sub> ) <sub>2</sub> ]					
R <sub>1</sub> = R <sub>2</sub> = Et, <i>i</i> -Pr, <i>n</i> -Bu, <i>i</i> -Bu		310–346 (CH <sub>2</sub> Cl <sub>2</sub> )			40
(R <sub>1</sub> , R <sub>2</sub> ) = (Et, <i>n</i> -Bu), ( <i>n</i> -Bu, <i>i</i> -Bu)		311–334 (CH <sub>2</sub> Cl <sub>2</sub> )			40
(R <sub>1</sub> , R <sub>2</sub> ) = –CHR <sub>4</sub> –CHR <sub>5</sub> –(CH <sub>2</sub> ) <sub>2</sub> –CHR <sub>6</sub> –] <sup>d</sup>		311–336 (CH <sub>2</sub> Cl <sub>2</sub> )			40

<sup>a</sup> In ppm referenced to 0.1 M aqueous Cd(ClO<sub>4</sub>)<sub>2</sub>. Chemical shifts in ref 38 were reported relative to 4.5 M Cd(NO<sub>3</sub>)<sub>2</sub> and have been corrected here to the former standard by subtracting 73 ppm from the published values. <sup>b</sup> Room temperature unless indicated. <sup>c</sup> *i*-MNT denotes [(NC)<sub>2</sub>C=CS<sub>2</sub>]<sup>2-</sup>. <sup>d</sup> (R<sub>4</sub>, R<sub>5</sub>, R<sub>6</sub>) = (H, H, H), (Me, H, H), (H, Me, H), (Me, H, Me).

**Table VIII.** Estimates for  $\sigma_{11}$  in Cadmium–Sulfur Complexes with Ligands Adopting the Stereochemistry Found in [NMe<sub>4</sub>][Cd(S<sub>2</sub>CSC<sub>6</sub>H<sub>11</sub>)<sub>3</sub>] (2)

site (geom) complex	tensor elements, ppm				$\sigma_{11}^{\text{est } a}$	no. of Cd–S vectors perpendicular to $\sigma_{11}$	$d(\text{Cd-S})$ av, $\text{\AA}$	ref
	$\sigma_{11}$	$\sigma_{22}$	$\sigma_{33}$	$\sigma_{\text{iso}}$				
CdS <sub>3</sub> (trig pl)								
[PPh <sub>4</sub> ][Cd(S-2,4,6- <i>i</i> -Pr <sub>3</sub> C <sub>6</sub> H <sub>2</sub> ) <sub>3</sub> ]	990	545	469	668	592	3	2.42	5
CdS <sub>4</sub> (tetr)								
[Cd(SC <sub>5</sub> H <sub>9</sub> NHMe) <sub>2</sub> ][ClO <sub>4</sub> ] <sub>2</sub> (3)	712	699	514	641	515	2	2.55	this work
CdS <sub>4</sub> (sq pl)								
[Cd( <i>i</i> -MNT) <sub>2</sub> ] <sup>2-</sup>	504	137	134	258	406	4	2.635	37
CdS <sub>4</sub> (tetr)								
[Cd(S <sub>2</sub> CO- <i>n</i> -Bu) <sub>2</sub> ]	550	455	329	445	420	2	2.59	28
[Cd(S <sub>2</sub> COEt) <sub>2</sub> ]	562	438	241	414	415	2	2.56	28
CdS <sub>6</sub> (dist trig prism)								
[NMe <sub>4</sub> ][Cd(S <sub>2</sub> CSC <sub>6</sub> H <sub>11</sub> ) <sub>3</sub> ] (2)	356	107	68	177			2.70	this work

<sup>a</sup> Calculated according to eq 2 (see text).

the Cd–S distance in **2** is also the longest of all complexes studied here (Table V).

The similarity between  $\sigma_{\text{iso}}$  in tris(dithio) complexes (Table VII) suggests that the specific nature of the sulfur-containing ligand is an essential determinant of the isotropic chemical shift. In order to validate this assumption, we have followed the theory developed by Ellis,<sup>27</sup> which allows us to estimate the tensor principal components as a function of M–L bond lengths and the relative orientation of these in the principal axis frame. Accordingly, in homoleptic complexes with axial symmetry the following relation holds:

$$\sigma_{11} = k\theta_s(\cos \phi)(R_{\text{Cd-S}})^{-3} \quad (1)$$

where  $k$  is a proportionality constant,  $\theta_s$  stands for the intrinsic shielding contribution from sulfur atoms in a given type of ligand,  $\phi$  is the angle that Cd–S vectors make with a plane perpendicular to  $\sigma_{11}$ , and  $R_{\text{Cd-S}}$  refers to the Cd–S bond length. Thus, these last two parameters act as geometric factors scaling the contribution of Cd–S bonds to the shielding of  $\sigma_{11}$ , which is maximum when the internuclear vectors are orthogonal ( $\cos \phi = 1$ ) to that principal axis. The evaluation of equivalent equations involving  $\sigma_{22}$  and  $\sigma_{33}$  would require single-crystal oriented <sup>113</sup>Cd NMR,

which affords the complete orientation of the tensor in the molecular reference frame.

In order to determine the influence of the nature of the ligand on the value of  $\sigma_{11}$ , eq 1 cannot be used directly, but eq 2 has been derived instead, where  $d(\text{Cd-S})_{(2)}$  and  $\phi_{(2)}$  correspond to values found at the CdS<sub>6</sub> (**2**) site and have been taken as 2.70 Å and 30°, respectively. This expression allows us to estimate the

$$\sigma_{11}^{\text{est}} = \sigma_{11}^{\text{ref}} \left[ \frac{d(\text{Cd-S})_{\text{ref}}}{d(\text{Cd-S})_{(2)}} \right]^3 \frac{\cos \phi_{(2)}}{\cos \phi_{\text{ref}}} \quad (2)$$

hypothetical value of the principal component  $\sigma_{11}^{\text{est}}$  corresponding to complexes with known structure (and thus with definite values for  $\sigma_{11}^{\text{ref}}$ ,  $d(\text{Cd-S})_{\text{ref}}$ , and  $\phi_{\text{ref}}$ ) if, preserving the same type of ligand, their stereochemistry around cadmium changed to that found at the CdS<sub>6</sub> (**2**) site. The five reference complexes selected for this purpose include different sulfur-containing ligands. Moreover,  $\phi = 0$  for all of them, as it is very likely that the  $\sigma_{11}$  principal axis is perpendicular to a different number of cadmium–sulfur bonds, these ranging from 2 to 4.  $\sigma_{11}^{\text{est}}$  for these reference complexes are given in Table VIII. As expected,  $\sigma_{11}^{\text{est}}$  values are smaller than  $\sigma_{11}^{\text{ref}}$  in all cases due to the longer Cd–S distance and approximately 30° angle of the CdS<sub>6</sub> (**2**) site. However,  $\sigma_{11}^{\text{est}}$  values for aliphatic and hindered aromatic thiols are still far from 356 ppm, corresponding to  $\sigma_{11}$  at the CdS<sub>6</sub> (**2**) site. Conversely,  $\sigma_{11}^{\text{est}}$  for *gem*-dithio ligands are much closer, 400–420 ppm, which indicates that these ligands have lower deshielding ability than conventional thiolates. Unfortunately, no cadmium complexes with four-membered CdS<sub>2</sub>X chelate rings including electron delocalization as in complex **2** have been studied by <sup>113</sup>Cd CP/MAS-NMR techniques. The bis(xanthato) complexes used as reference (Table VIII) might apparently meet these require-

(36) Domenicano, A.; Torelli, L.; Vacicago, A.; Zambonelli, L. *J. Chem. Soc. A* **1968**, 1351.

(37) Li, H. Y.; Amma, E. L. *Inorg. Chim. Acta* **1990**, *177*, 5.

(38) Abrahams, B. F.; Winter, G.; Dakternieks, D. *Inorg. Chim. Acta* **1989**, *162*, 211.

(39) McCleverty, J. A.; Gill, S.; Kowalski, R. S. Z.; Bailey, N. A.; Adams, H.; Lumbard, K. W.; Murphy, M. A. *J. Chem. Soc., Dalton Trans.* **1982**, 493.

(40) Bond, A. M.; Colton, R.; Dakternieks, D.; Dillon, M. L.; Hauenstein, J.; Moir, J. E. *Aust. J. Chem.* **1981**, *34*, 1393.

(41) Lawton, S. L.; Kokotailo, G. T. *Inorg. Chem.* **1969**, *8*, 2410.

(42) Casas, J. S.; Sánchez, A.; Bravo, J.; García-Fontán, S.; Castellano, E. E.; Jones, M. M. *Inorg. Chim. Acta* **1989**, *158*, 119.

ments, but their structure is polymeric and they do not contain chelate rings. Lack of quantitative estimates for  $\sigma_{22}^{\text{est}}$  and  $\sigma_{33}^{\text{est}}$  prevents extending previous arguments to  $\sigma_{\text{iso}}$  values, although it seems reasonable to suppose that the former follow the trend observed for  $\sigma_{11}^{\text{est}}$ . This is supported by the fact that the experimental values for  $\sigma_{22}$  and  $\sigma_{33}$  at the  $\text{CdS}_6$  (2) site are among the lowest tensor principal components in Table IV.

### Conclusions

Seven cadmium–sulfur complexes, including nine different cadmium sites, have been studied by solid  $^{113}\text{Cd}$  NMR and compared to previous solid-state or single-crystal oriented NMR reports. The structure of two complexes is here reported, while that of the rest have previously been determined by X-ray diffraction.

In the first stage the shielding tensor parameters  $\eta$  (asymmetry) and  $\Delta\sigma$  (anisotropy) were related to the stereochemistry around cadmium, allowing us to derive two main conclusions. First, when constraints are imposed on the cadmium site by crystallographic or idealized local symmetry, the value found for  $\eta$  is low. As expected, in the absence of appropriate symmetry elements on the cadmium atom  $\eta$  increases except for two sites, where the lack of symmetry is not reflected in this parameter. Second,  $\Delta\sigma$  agrees well with the geometry around the cadmium atom. Hence, those sites whose symmetry does not depart significantly from that of a regular polyhedron show  $\Delta\sigma$  values ranging from 200 to 300 ppm. Marked distortions from a regular geometry give rise to clearly higher values. Moreover, although all existing information indicates that the isotropic cadmium chemical shift,  $\sigma_{\text{iso}}$ , is not sufficiently discriminating to allow well-established structure–shift correlations, shielding increases in the sequence  $\text{S} < \text{Cl} < \text{Br} < \text{N}$ .

In the second stage, the structure–shift correlations were extended to the individual elements of the tensor. This requires a previous orientation of the shielding tensor in the molecular reference frame, which was accomplished by applying two main criteria relative to the influence of the stereochemistry around

cadmium on shielding tensor individual components. These criteria are that the shielding effects of a given M–L bond are maximal in the directions perpendicular to the M–L vector and that sulfur is the most deshielding donor atom. Accordingly, on the basis of the structural features and  $\sigma_{11}$ ,  $\sigma_{22}$ , and  $\sigma_{33}$  values corresponding to a particular cadmium site, four different tensor–molecular frame orientations were proposed for the nine distinct  $^{113}\text{Cd}$  shielding tensors. One particular orientation was assigned to the five slightly distorted tetrahedral cadmium sites:  $\text{CdS}_4$  (1 and 3) and  $\text{CdS}_2\text{X}_2$ ,  $\text{X} = \text{Cl}$  (4) or  $\text{Br}$  (5 and 6). Another orientation was common for the octahedral  $\text{CdS}_2\text{N}_2\text{Cl}_2$  (7) site and for the  $\text{CdS}_2\text{N}_2\cdots\text{Br}_2$  (6) site that is tetrahedral with severe distortion toward octahedral. The remaining two orientations were respectively associated with the twisted trigonal prism ( $\text{CdS}_6$  (2)) and distorted trigonal-bipyramid ( $\text{CdS}_3\text{N}\cdots\text{Cl}$  (7)) geometries. For each of the four coordination types, the assigned orientation has allowed us to compare similar sites in different complexes. Also, variations in the individual tensor components have been satisfactorily related to changes in geometric parameters around the cadmium atom.

Finally, a semiquantitative analysis of the low value of the  $\sigma_{11}$  tensor component in the  $\text{CdS}_6$  site of the tris(cyclohexylthioanthato)cadmate anion (2) has enabled us to conclude that, although sulfur atoms are known to have a marked deshielding ability, this property is strongly modulated by the specific nature of the sulfur-containing ligand. Thus, deshielding effects of sulfur in *gem*-dithio ligands have been found to be significantly lower than in simple thiolates.

**Acknowledgment.** We thank the Ministerio de Educación y Ciencia (DGICYT, PB90-0691) for financial support.

**Supplementary Material Available:** Tables of atomic coordinates, thermal parameters, bond distances and angles, and hydrogen atom positions for 1 and 2 (15 pages); tables of observed and calculated structure factors for 1 and 2 (35 pages). Ordering information is given on any current masthead page.